

## Benzene Intermediates and Mechanisms during Catalytic Oxidation on the Pt(111) Surface Using In-Situ Soft X-ray Methods

Anderson L. Marsh,<sup>†</sup> Daniel J. Burnett,<sup>‡</sup> Daniel A. Fischer,<sup>§</sup> and John L. Gland<sup>\*,†,‡</sup>

Department of Chemistry and Department of Chemical Engineering, University of Michigan, Ann Arbor, Michigan 48109, and Materials Science and Engineering Laboratory, National Institute of Standards and Technology, Gaithersburg, Maryland 20899

Received: February 17, 2003; In Final Form: July 16, 2003

The catalytic oxidation of benzene on the Pt(111) surface has been characterized, in flowing oxygen pressures up to 0.01 Torr, using temperature-programmed fluorescence yield near-edge spectroscopy (TP-FYNES). During temperature-programmed oxidation experiments in flowing oxygen pressures, a series of four adsorbed intermediates are formed. The dominant intermediates with increasing temperature are  $\eta^6$ -benzene, 1,4-di- $\sigma$ -2,5-cyclohexadiene, 1,1,4-tri- $\sigma$ -2,5-cyclohexadiene, and  $\eta^5$ -cyclohexadienone. All of these intermediates are strongly adsorbed based on the molecular rehybridization indicated by spectroscopic (FYNES) measurements. Adsorbed benzene inhibits oxidation below 370 K by inhibiting oxygen adsorption. Over the temperature range 150–215 K, a 1,4-di- $\sigma$ -2,5-cyclohexadiene surface intermediate with  $C_6H_6$  stoichiometry is formed by rearrangement of the aromatic ring. Next, a 1,1,4-tri- $\sigma$ -2,5-cyclohexadiene surface intermediate with  $C_6H_5$  stoichiometry is formed by oxydehydrogenation over the temperature range 215–285 K. Above 350 K, a fraction of this intermediate is oxidized to form carbon dioxide and water, while the remainder is oxygenated to form a  $\eta^5$ -cyclohexadienone intermediate with  $C_6H_5O$  stoichiometry, which is dominant at 390 K. The reactivity of this intermediate is clearly demonstrated by rapid oxidation with increasing temperature. No change in the onset temperature for rapid oxidation or the rate of carbon removal is observed with increasing oxygen pressures over the pressure range 0.0005–0.01 Torr. Temperature-programmed reaction spectroscopy (TPRS) has been used to identify the gas-phase products during deep oxidation between coadsorbed benzene and oxygen on Pt(111). Carbon dioxide and water are formed over the 300–500 K temperature range when benzene is in excess, and over the 380–620 K temperature range when oxygen is in excess. This combination of temperature-programmed UHV and in-situ soft X-ray methods has provided a detailed mechanistic description of catalytic benzene oxidation on the Pt(111) surface.

### Introduction

Transition metal catalysts are used in many industrial processes to efficiently synthesize desired products and to remove unwanted contaminants.<sup>1</sup> For example, platinum, along with palladium and rhodium, is used in the automotive industry as a catalyst to remove carbon monoxide and unburned hydrocarbons from exhaust. Modern surface science has focused on exploring and understanding catalytic reactions to establish a molecular-level understanding of fundamental surface processes.<sup>2</sup> Surface structures and active sites are identified through the use of simplified model systems, such as single-crystal surfaces. Using carefully selected combinations of surface science techniques to provide molecular-level information on the elementary reaction steps, mechanisms are characterized. Most of the work performed to date has been done under ultrahigh vacuum (UHV) conditions, since many surface-sensitive spectroscopies require the detection of electrons. However, techniques have been developed to characterize catalytic reactions on model surfaces at a molecular level in

elevated pressures.<sup>3–5</sup> Reactions are probed in-situ using single-crystal surfaces as model catalysts, and afterward the surface is characterized using standard UHV techniques. These studies have shown that some catalytic reactions have different mechanisms under UHV and elevated-pressure conditions. Thus, a more complete understanding of reaction mechanisms is gained from investigations done over a wide range of pressure conditions.

On noble metal catalysts, a Langmuir–Hinshelwood mechanism is generally observed for the deep catalytic oxidation of nucleophilic organics.<sup>6</sup> The first step of the mechanism is the adsorption of molecular oxygen and its rapid dissociation to form atomic oxygen. In the next step, an adsorbed organic molecule reacts with the surface oxygen. Several different mechanisms have been proposed for the deep catalytic oxidation of benzene on platinum catalysts. On  $\gamma$ -alumina supported platinum catalysts, the Mars-van Krevelen mechanism has been suggested as a model to describe benzene oxidation.<sup>7–10</sup> In this case, gas-phase benzene reacts with the oxidized catalyst to give a reduced catalyst and the products. Gas-phase oxygen then reacts with the reduced catalyst to regenerate an oxidized catalyst. Under different experimental conditions a Langmuir–Hinshelwood mechanism has been proposed for benzene oxidation over a Pt–Al<sub>2</sub>O<sub>3</sub> catalyst.<sup>11</sup> In this situation, benzene is rapidly and strongly adsorbed on metallic platinum. This strong

\* Author to whom correspondence should be addressed at University of Michigan, 930 N. University Ave., Ann Arbor, MI 48109. Phone: 734-764-7354. Fax: 734-647-4865. E-mail: gland@umich.edu.

<sup>†</sup> Department of Chemistry, University of Michigan.

<sup>‡</sup> Department of Chemical Engineering, University of Michigan.

<sup>§</sup> Materials Science and Engineering Laboratory, National Institute of Standards and Technology.

adsorption inhibits oxygen adsorption, thus inhibiting combustion. In another study, a highly reactive surface-bound phenyl species has been proposed as an intermediate during benzene oxidation over an alumina-supported platinum catalyst.<sup>12</sup> This conclusion is based on comparison of isotope experiments involving benzene and chlorobenzene. In addition, on the basis of the kinetic isotope experiments, carbon–hydrogen bond activation is proposed to be rate-determining for this reaction. These authors also found that oxidation is zero-order in oxygen at high oxygen concentrations. For metallic platinum, two reaction paths with differing oxidation intermediates have been considered for the complete oxidation of benzene.<sup>13–14</sup> One path involves the reaction of adsorbed oxygen with adsorbed benzene, while the second path involves the reaction of adsorbed benzene with gas-phase oxygen. Although benzene catalytic oxidation has been thoroughly investigated, discrepancies exist with regard to the overall mechanism. Molecular-level characterizations based on single-crystal model catalyst surfaces provide a better mechanistic description; yet, they have not been performed as extensively for benzene oxidation.

The interactions of benzene with the Pt(111) surface have been studied in detail using a variety of surface science techniques.<sup>15–25</sup> On the basis of these results, benzene  $\pi$ -bonds with the ring parallel to the plane of the surface, and a saturated surface coverage consists of two chemisorbed states which are desorbed with activation energies of 82–88 kJ/mol and 117–129 kJ/mol over the 280–520 K temperature range.<sup>15–17,19,22</sup> The preferred site for benzene adsorption is the bridge site, which is occupied first during adsorption and has an adsorption energy of 117 kJ/mol, while at higher coverages a 3-fold hollow site, which has an adsorption energy of 75 kJ/mol, is occupied.<sup>25</sup> In addition to these studies of benzene adsorption on the Pt(111) surface, the deep oxidation of benzene on several transition metal surfaces has been investigated under UHV conditions.<sup>26–30</sup> The reaction of benzene with preadsorbed atomic oxygen on a 10 nm platinum thin film, supported on aluminum oxide, has been characterized using temperature-programmed reaction spectroscopy (TPRS) over a range of benzene coverages.<sup>27</sup> Even with excess atomic oxygen, a fraction of the benzene is desorbed molecularly over the 200–400 K temperature range, while all strongly adsorbed benzene remaining on the surface is oxidized. Both CO<sub>2</sub> and H<sub>2</sub>O formed by oxidation are desorbed over the 300 to 500 K temperature range. The oxidation of benzene by preadsorbed atomic oxygen on the Pd(111) surface has been studied using TPRS over a range of atomic oxygen coverages.<sup>28</sup> The reaction products formed are carbon dioxide, water, and carbon monoxide, and all three molecules are desorbed over the 400–600 K temperature range. Chemisorbed benzene is desorbed in a broad peak from 200 to 600 K. For initial atomic oxygen coverages above 0.34 ML, little benzene is adsorbed on the oxygen-saturated surface, which suppresses CO<sub>2</sub> and H<sub>2</sub>O formation. We have previously reported on the mechanisms of benzene oxidation on the Pt(111) surface under UHV conditions using temperature-programmed reaction methods.<sup>30</sup> Benzene is oxidized to produce carbon dioxide and water, which desorb from 300 to 500 K. Carbon–hydrogen and carbon–carbon bond activation are clearly rate-limiting steps for carbon dioxide and water formation. The intensity of the high-temperature benzene desorption peak (425 K) decreases with increasing oxygen coverage, suggesting enhanced reactivity of the corresponding bridge-bonded configuration.

To connect studies of deep oxidation on platinum catalysts with those on model surfaces under UHV conditions, we have applied a combination of soft X-ray absorption spectroscopies

at the C-K-edge to characterize benzene catalytic oxidation on the Pt(111) surface. These methods have been used previously to characterize light hydrocarbon oxidation mechanisms on the Pt(111) surface in flowing oxygen pressures.<sup>31–33</sup> In this work, fluorescence yield near-edge spectroscopy (FYNES) and temperature-programmed FYNES (TP-FYNES) have been used to characterize the deep oxidation of benzene in flowing oxygen pressures up to 0.01 Torr. With increasing temperature, a series of four intermediates are formed on the surface during oxidation. Below 150 K, benzene is adsorbed on the Pt(111) surface in a  $\eta^6$ -configuration that results in the rehybridization of the aromatic system and tilting of the C–H bonds away from the surface plane. Over the 150–285 K temperature range, a C<sub>6</sub>H<sub>5</sub> 1,1,4-tri- $\sigma$ -2,5-cyclohexadiene intermediate is formed on the surface by rearrangement of the aromatic ring and subsequent oxydehydrogenation. Above 370 K the surface intermediate rapidly reacts with surface oxygen to produce a clean surface by 450 K. On the basis of spectroscopic measurements at 390 K, the dominant hydrocarbon intermediate in this temperature range is C<sub>6</sub>H<sub>5</sub>O  $\eta^5$ -cyclohexadienone. In connection with these experiments in pressures of flowing oxygen, CO<sub>2</sub> and H<sub>2</sub>O have been identified as the gas-phase oxidation products using TPRS. Both temperature-programmed UHV and elevated-pressure oxidation experiments have supplied in-depth information on the mechanisms and intermediates for benzene catalytic oxidation on the Pt(111) surface.

## Experimental Section

The soft X-ray experiments were performed in the surface science endstation on the U7A beamline at the National Synchrotron Light Source (NSLS) located at Brookhaven National Laboratory. These experiments and the experimental setup have been described in detail previously.<sup>31</sup> The upper chamber (where these experiments were conducted) consists of two smaller chambers separated by a window valve equipped with a 2000 Å Al window, which is approximately 20% transparent at 330 eV. The window remains out for vacuum experiments and is inserted when experiments are conducted in flowing oxygen pressures. The Pt(111) crystal was mounted on Ta wire supports at the end of a 6-ft liquid nitrogen cooled re-entrant manipulator insert. Temperature was measured with a Type K thermocouple spot-welded to the back of the crystal and was controlled with a RHK temperature controller. The crystal was cleaned in the lower chamber by initial Ar<sup>+</sup> sputtering, followed by annealing briefly at 1000 K. During experimental runs, the sample was cleaned by heating the crystal at 600 K in 0.002 Torr of oxygen for 60 s, followed by a 10 s exposure to carbon monoxide. Reactive gases were admitted to the background through variable leak valves.

FYNES and TP-FYNES experiments were performed using a proportional counter optimized for fluorescence detection at the C-K-edge.<sup>34</sup> Fluorescence yield spectra were collected with 150  $\mu$ m/150  $\mu$ m slits, giving an overall resolution of 0.4 eV. All spectra of adsorbed species have been divided by spectra of the clean surface taken on the same ring fill to ensure reproducibility. Spectra of adsorbed species were recorded at 100 K (benzene) and 350 K (oxidation intermediate), while spectra of the clean surface were recorded at 500 K to limit CO adsorption from the background. The temperature-programmed oxidation experiments were performed with 450  $\mu$ m/450  $\mu$ m slits, giving an overall resolution of 1.2 eV and an intensity of 10 000 counts/s for a saturated CO coverage with the window inserted. Data were averaged over a 4 s interval, which results in a signal-to-noise ratio of about 4 to 1 for a saturated CO coverage. The

heating rate was 0.5 K/s during these temperature-programmed experiments.

TP-FYNES experiments and preparation of surface species were conducted in the following manner. After the crystal was cleaned and cooled to 170 K, a saturated coverage of benzene was dosed. Once the surface carbon concentration reached the saturation level, the leak valve was closed and the crystal was cooled to 150 K. Next, oxygen was introduced, the ion gauge was turned off, and the ultimate pressure was achieved by a combination of throttling the gate valve in front of the turbo pump and controlling the leak valve while monitoring the pressure with a 1 Torr capacitance manometer. Throttling the turbo pump resulted in a flowing system with 10% flow. CO TP-FYNES was used to confirm the performance of this system and reproduce published results. Repeated experiments with benzene indicate thermal transitions are reproducible to 2 K. Absolute carbon coverage for benzene was estimated by comparing the carbon continuum levels observed during these experiments and experiments with a saturated CO coverage. Since the absolute carbon coverage for a saturated CO coverage is known to be  $9.6 \times 10^{14}$  molecules/cm<sup>2</sup>, it is possible to estimate absolute surface carbon concentration for any carbon-containing adsorbed species.<sup>35</sup>

The TPRS experiments were conducted in the Ann Arbor ultrahigh vacuum (UHV) chamber at the University of Michigan, which has also been described in detail previously.<sup>30</sup> The crystal was cleaned by cycles of Ar<sup>+</sup> sputtering and annealing in background pressures of oxygen. Surface cleanliness was verified by Auger electron spectroscopy (AES) and oxygen temperature-programmed desorption (TPD). The experiments were performed using a UTI 100C mass spectrometer interfaced with a PC. A heating rate of 5 K/s was used for these experiments. Initially, the benzene (Baker Analyzed) was purified by freeze–pump–thawing several times, and the purity was checked by mass spectrometry. After that, the benzene was freeze–pump–thawed at the start of each set of experiments. The reactive gases were directly dosed using stainless steel capillaries and variable leak valves. For oxygen exposures the crystal was placed 5 mm away from the doser, while for benzene exposures the crystal was placed 25 mm away from the doser. All gas exposures for TPRS were performed with the crystal temperature below 100 K. Saturated atomic oxygen coverages were prepared by heating saturated coverages of molecular oxygen to 150 K. All pressures are given in units of Torr, where 1 Torr = 1.333 mbar = 133.322 Pa.

## Results

The adsorption and bonding of benzene on the Pt(111) surface has been characterized using FYNES. Spectra shown in Figure 1 were collected at normal (90°) and glancing (30°) incidences of the electric field vector with respect to the surface normal. Both spectra were normalized to zero fluorescence yield below 280 eV and to a constant fluorescence yield at 330 eV. The spectra were curve fit after subtracting a step function (shown as a dashed curve) placed at a position of 290.1 eV and used to simulate the adsorption edge. This absorption step is a crude approximation for the density of states, but is used to simplify the curve-fitting process. Both spectra were curve fit using identical step functions, peak energies, and peak widths. Details of the curve-fitting procedure are found in the literature.<sup>36</sup> Each spectrum consists of five resonances resulting from transitions from the C 1s orbital to unfilled valence orbitals. The first four peaks have been assigned to the following resonances:  $\pi^*_{1,2}$  (284.8 eV), C–H  $\sigma^* + \pi^*_3$  (287.8 eV),  $\sigma^*_1$  (292.3 eV), and

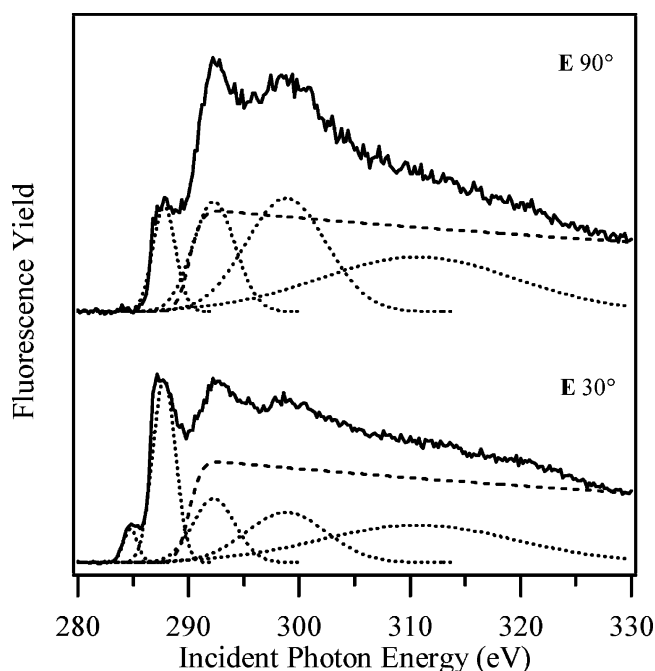


**Figure 1.** FYNES, recorded at normal (90°) and glancing (30°) incidences, of a saturated coverage of  $\eta^6$ -benzene adsorbed on the Pt(111) surface.

**TABLE 1: FYNES Resonance Assignments for  $\eta^6$ -Benzene Adsorbed on the Pt(111) Surface**

energy (eV)	resonance
284.8	$\pi^*_{1,2}$
287.8	C–H $\sigma^* + \pi^*_3$
292.3	$\sigma^*_1$
298.8	$\sigma^*_2$
310.7	multiple scattering

$\sigma^*_2$  (298.8 eV). The peak at 310.7 eV has been assigned to a multiple scattering resonance, as previously done for propylene adsorbed on the Pt(111) surface.<sup>31</sup> Above 330 eV, the fluorescence yield is solely the result of transitions from the C 1s orbital to the carbon continuum. The resonance assignments in this work have been summarized in Table 1 and are based on previous work involving benzene adsorbed on the Pt(111)<sup>18</sup> and Ag(110)<sup>37</sup> surfaces. Tilt angles for chemical bonds in adsorbed species are calculated on the basis of the intensity ratio for resonances in spectra collected at two different angles of incidence.<sup>38</sup> The peak intensity of the  $\pi^*_{1,2}$  resonance in the spectrum for normal incidence is lower than the peak intensity in the spectrum for glancing incidence. Using the intensity ratio  $I_{90^\circ}/I_{30^\circ}$  and a polarization factor of 0.85, a tilt angle of  $11^\circ \pm 2^\circ$  relative to the surface normal has been calculated for the  $\pi^*_{1,2}$  orbital. The same calculation has been done for the C–H  $\sigma^*$  resonance. The peak intensity in the spectrum for normal incidence is higher than the peak intensity in the spectrum for glancing incidence. A tilt angle of  $46^\circ \pm 5^\circ$  relative to the surface normal has been calculated for this orbital.

The deep catalytic oxidation of benzene in pressures of flowing oxygen has been characterized using TP-FYNES. Pressures of 0.0005, 0.002, and 0.01 Torr oxygen were used. These experiments were performed at 330 eV and at normal incidence. As indicated in the previous paragraph, at this energy the fluorescence yield is a direct measure of the amount of carbon adsorbed on the surface and the intensity is independent of orientation. As seen in Figure 2, the carbon coverage is monitored while heating a saturated coverage of benzene in a



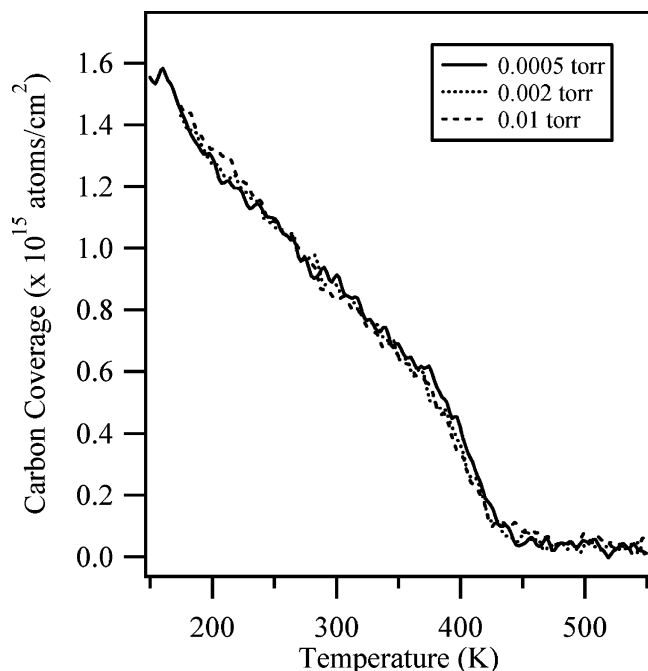


**Figure 2.** TP-FYNES recorded at the carbon continuum (330 eV) for the oxidation of a saturated coverage of benzene as a function of increasing flowing oxygen pressure.

pressure of flowing oxygen. These spectra were normalized first by setting the intensity above 450 K to zero carbon coverage, then by setting the intensity at 150 K equal to the carbon coverage for a saturated benzene coverage. A saturated coverage of benzene corresponds to  $1.55 \times 10^{15}$  C atoms/cm<sup>2</sup> (or  $2.58 \times 10^{14}$  molecules/cm<sup>2</sup>) based on direct comparison with the fluorescence yield for a saturated coverage of CO. The initial decrease in carbon coverage is gradual and occurs from 175 to 370 K. This decrease corresponds to the removal of  $9.5 \times 10^{14}$  C atoms/cm<sup>2</sup>, or 60% of the carbon coverage. In the presence of oxygen the carbon coverage rapidly decreases to zero over the temperature range 370 to 450 K. No significant change, in the rate of carbon removal or onset temperature for rapid oxidation, is observed with an increase in oxygen pressure.

The products of the deep oxidation of benzene by coadsorbed atomic oxygen have been identified using TPRS. The transition from excess benzene to excess oxygen is shown in Figure 3. As shown in the mass 78 spectrum for the condition of excess benzene, the low-temperature chemisorbed state (3-fold hollow site) is desorbed in a peak at 320 K, and is finished desorbing by 400 K. A small amount of bridge-bonded benzene is desorbed in a peak at 500 K, and is finished desorbing by 540 K. The major products desorbed from the surface are carbon dioxide (mass 44 spectrum) and water (mass 18 spectrum). No significant concentrations of carbon monoxide were detected. The initial water desorption peak below 300 K results primarily from oxygen reacting with adsorbed background hydrogen and from adsorbed background water. The complete oxidation products, CO<sub>2</sub> and H<sub>2</sub>O, are desorbed between 300 and 500 K when benzene is in excess. For the condition of excess oxygen on the surface, carbon dioxide and water desorb from 380 to 620 K. For excess benzene, once the oxygen has been consumed by reaction the remaining benzene is dehydrogenated to produce adsorbed carbon, and hydrogen, which is desorbed in two peaks, as seen in the mass 2 spectrum. Both H<sub>2</sub> peaks, one at 520 K and one at 635 K, are similar in temperature and shape to those in the spectrum for chemisorbed benzene without preadsorbed oxygen.<sup>16,19,22</sup> No peaks are observed in either the mass 2 or

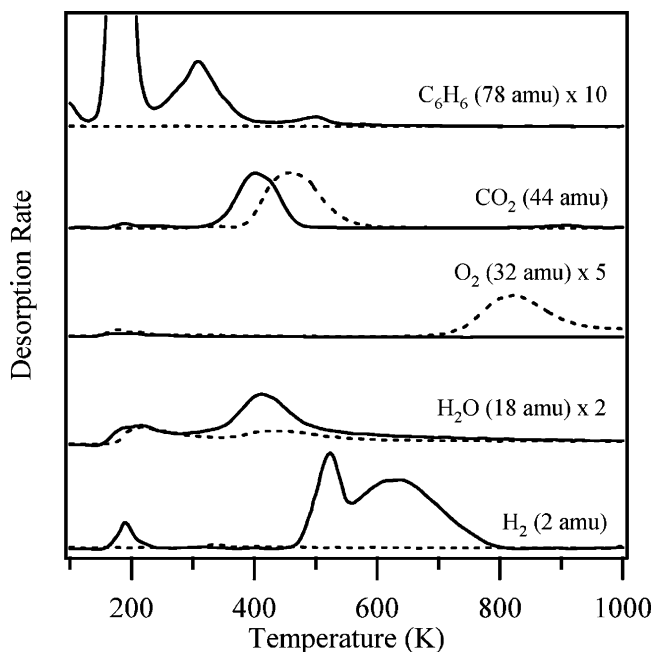
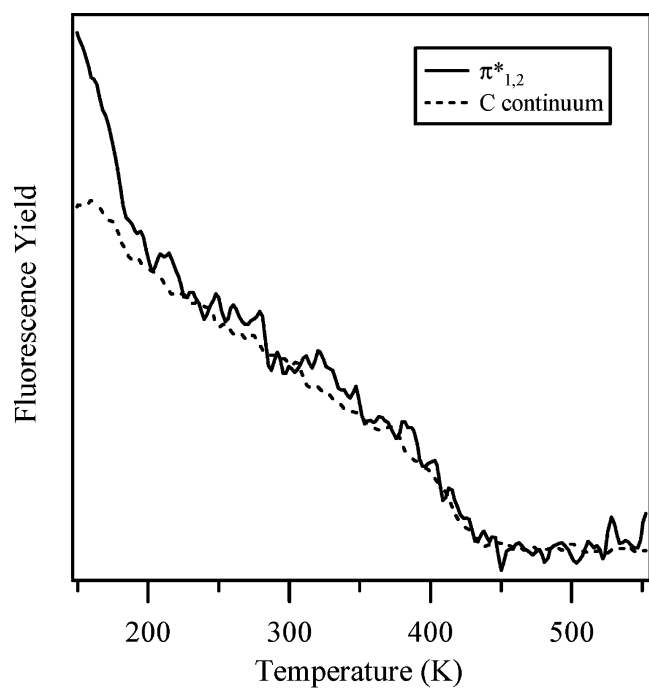


**Figure 3.** TPRS spectra of benzene oxidation on the Pt(111) surface for the conditions of excess benzene (—) and excess oxygen (---).

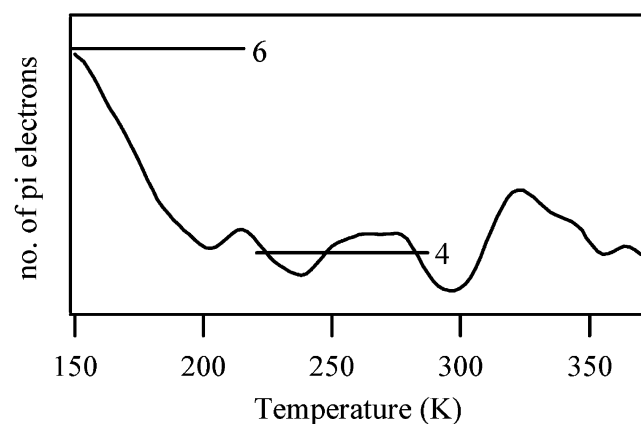
the mass 78 spectrum when oxygen is in excess. Remaining atomic oxygen recombines and desorbs above 700 K for this benzene coverage. Experiments have also been performed to determine the structure and stoichiometry of surface intermediates present during complete benzene oxidation on the Pt(111) surface.

To determine the structure of the aromatic ring during oxidation, experiments were conducted in which the intensity of the  $\pi^*_{1,2}$  resonance (284.8 eV) was followed at an angle of incidence of 55°. At this “magic” angle resonance intensities are independent of molecular orientation on the surface.<sup>39</sup> In addition, since this resonance falls below the absorption step there are no ambiguities related to overlap with the carbon continuum. The intensity of the C continuum (330 eV) as a function of temperature was also determined using the same angle of incidence. For these experiments, saturated coverages of benzene were heated in 0.002 Torr of flowing oxygen. For both spectra in Figure 4a the intensity above 450 K has been normalized to zero. As clearly shown by the results in Figure 4a, the spectrum corresponding to the  $\pi^*_{1,2}$  resonance shows an initial, steep drop in intensity below 215 K. No similar drop in intensity is observed in the spectrum corresponding to the carbon coverage (the C continuum). From 215 to 370 K the intensities of both spectra gradually decrease, then rapidly drop to zero by 450 K. The number of  $\pi$  electrons in each molecule is determined by taking the ratio of the  $\pi^*_{1,2}$  resonance to the surface carbon coverage (carbon continuum resonance). Figure 4b displays the  $\pi^*_{1,2}$  resonance spectrum divided by the C continuum spectrum. There is a decrease in the ratio below 215 K, then a constant level until 370 K. The initial ratio in Figure 4b has been normalized to 6  $\pi$  electrons, so this decrease corresponds to a drop in intensity from 6 to 4  $\pi$  electrons.

The C–H stoichiometry during oxidation was established by temperature-programmed experiments conducted to measure the intensity of the C–H  $\sigma^*$  resonance (287.8 eV) at an angle of 55°. As mentioned before, for these experiments, saturated coverages of benzene were heated in 0.002 Torr of flowing oxygen. The results for this C–H stoichiometry determination are presented in Figure 5. Both spectra in Figure 5a were normalized using the procedure mentioned in the previous



(a)

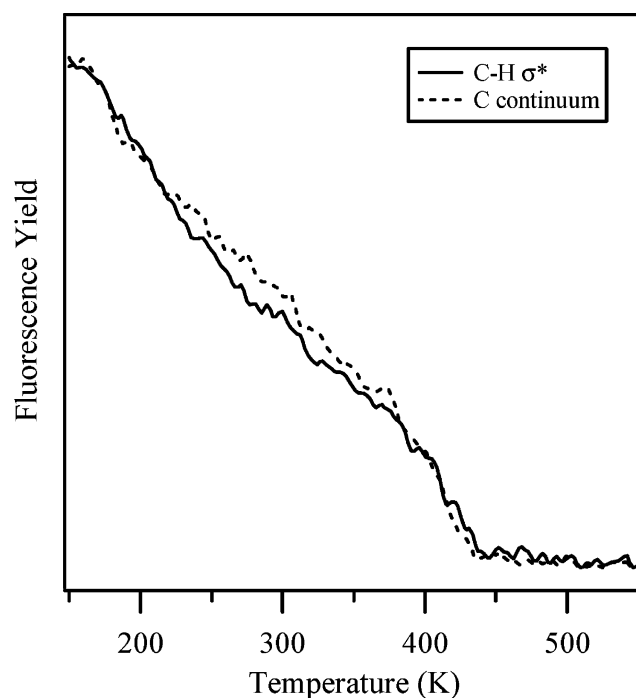


(b)

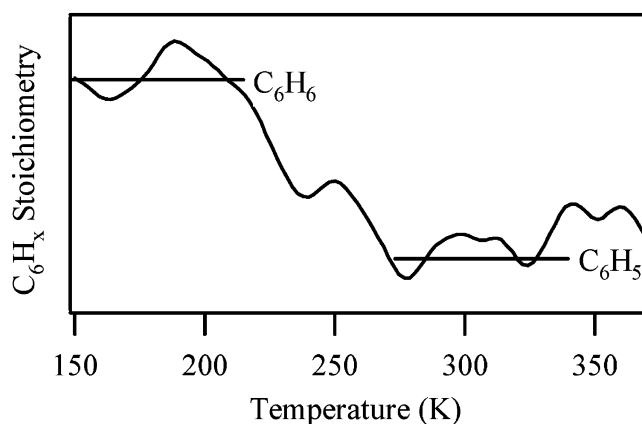
**Figure 4.** (a) TP-FYNES recorded at the  $\pi^*_{1,2}$  (284.8 eV) and carbon continuum (330 eV) energies during the oxidation of a saturated coverage of benzene in 0.002 Torr of flowing oxygen. (b) Ratio of the  $\pi^*_{1,2}$  spectrum (284.8 eV) to the carbon continuum (330 eV) spectrum.

paragraph. As clearly shown in Figure 5a by the spectrum corresponding to the C–H  $\sigma^*$  resonance, a gradual drop in intensity occurs below 215 K. A similar drop in intensity is also observed in the spectrum corresponding to the C continuum. Above 215 K, however, a drop in the intensity of the C–H  $\sigma^*$  resonance occurs that does not occur for the C continuum. The molecular C–H stoichiometry is determined by taking the ratio of the C–H  $\sigma^*$  resonance to the surface carbon coverage (carbon continuum resonance). Figure 5b shows the C–H  $\sigma^*$  resonance spectrum divided by the C continuum spectrum. There is a constant level below 215 K, then a decrease in the ratio from 215 to 285 K. Above 285 K the intensity ratio remains constant until 370 K. The initial ratio in Figure 5b has been normalized to 6 C–H bonds, so this decrease corresponds to a drop in intensity from 6 to 5 C–H bonds, or a change in stoichiometry from  $C_6H_6$  to  $C_6H_5$ .

In addition to these temperature-programmed stoichiometry measurements, the structure of the oxidation intermediate above 370 K has been characterized using FYNES. The intermediate



(a)



(b)

**Figure 5.** (a) TP-FYNES recorded at the C–H  $\sigma^*$  (287.8 eV) and carbon continuum (330 eV) energies during the oxidation of a saturated coverage of benzene in 0.002 Torr flowing oxygen. (b) Ratio of the C–H  $\sigma^*$  (287.8 eV) spectrum to the carbon continuum (330 eV) spectrum.

was prepared by heating a saturated coverage of benzene in 0.002 Torr of flowing oxygen to 390 K, then removing the oxygen and cooling the crystal to 350 K. The spectrum shown in Figure 6 was collected at 350 K and at normal ( $90^\circ$ ) incidence of the electric field vector with respect to the surface normal. The spectrum was normalized to zero fluorescence yield below 280 eV. The spectrum was fit after subtracting a step function (shown as a dashed curve) placed at a position of 289.8 eV and used to simulate the adsorption edge. This decrease in energy of 0.3 eV for the adsorption edge is similar to the difference in the C1s binding energy measured by XPS for dehydrogenated phenol adsorbed on the Pt(111) surface compared to benzene adsorbed on the Pt(111) surface.<sup>19,40</sup> The spectrum consists of six resonances resulting from transitions from the C 1s orbital to unfilled valence orbitals. The peaks have been assigned to the following resonances: C=C  $\pi^*$  (284.0 eV), C=O  $\pi^*$  (286.8 eV), C–H  $\sigma^*$  (288.2 eV),  $\sigma^*_1$  (292.6 eV),  $\sigma^*_2$  (298.7 eV). As done with the spectra for adsorbed benzene, the peak at 309.2

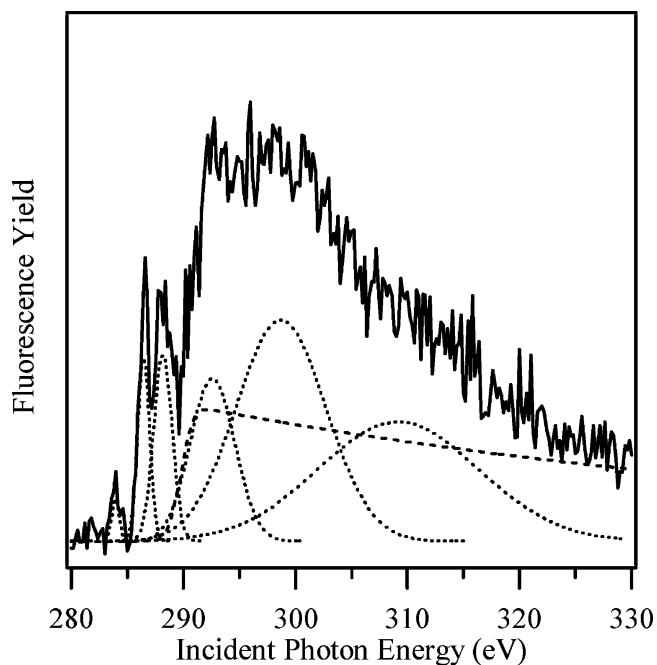


**Figure 6.** FYNES of  $\eta^5$ -cyclohexadienone adsorbed on the Pt(111) surface.

**TABLE 2: FYNES Resonance Assignments for  $\eta^5$ -Cyclohexadienone Adsorbed on the Pt(111) Surface**

energy (eV)	resonance
284.0	C=C $\pi^*$
286.5	C=O $\pi^*$
288.2	C-H $\sigma^*$
292.6	$\sigma^*_{1,2}$
298.7	$\sigma^*_{1,2}$
309.2	multiple scattering

eV has been assigned to a multiple scattering resonance. These resonance assignments have been summarized in Table 2 and are based on previous work involving benzene adsorbed on the Pt(111) surface,<sup>18</sup> benzene and phenol adsorbed on the Ag(110) surface,<sup>37</sup> and quinoid molecules.<sup>41–42</sup> The structural determinations have been combined with the temperature-programmed oxidation experiments to develop a complete mechanistic description of benzene catalytic oxidation on the Pt(111) surface.

## Discussion

The catalytic oxidation of benzene on the Pt(111) surface has been characterized in flowing oxygen pressures ranging from 0.0005 to 0.01 Torr using a combination of in-situ soft X-ray methods. FYNES indicates that benzene rehybridizes upon adsorption on the Pt(111) surface. Spectroscopic and temperature-programmed stoichiometric experiments clearly show that the deep oxidation of benzene proceeds through four surface intermediates. A mechanism has been developed on the basis of the combination of elevated-pressure and UHV experiments.

The structure of benzene adsorbed on the Pt(111) surface has been characterized using FYNES. Changes within the molecular structure of benzene are observed based on the fluorescence yield spectra. The tilt angle of the  $\pi^*_{1,2}$  orbital with respect to the surface normal is calculated to be  $11^\circ \pm 2^\circ$ . This calculated tilt angle suggests that the aromatic ring is adsorbed at an angle of  $11^\circ \pm 2^\circ$  with respect to the surface plane. For benzene adsorbed with the ring parallel to the plane of the surface, a tilt angle of  $0^\circ$  should be observed, as suggested by HREELS.<sup>15</sup> Using NEXAFS a tilt angle of  $18^\circ$  from the plane of the surface

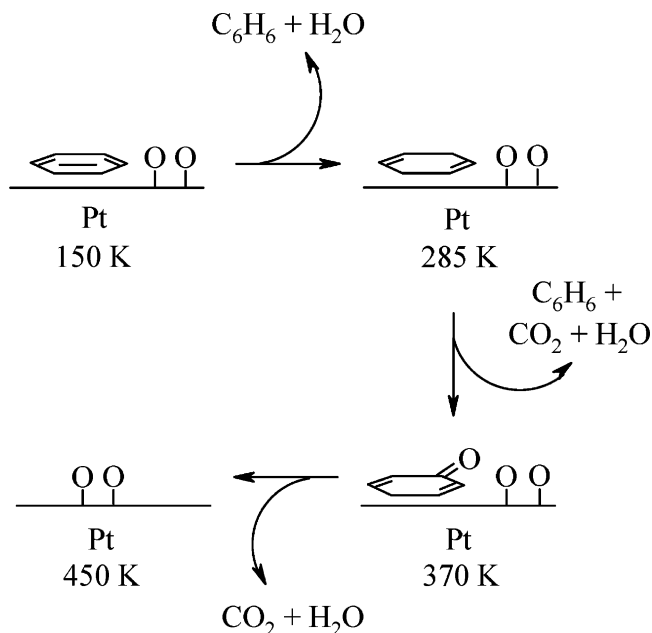


**Figure 7.** Mechanism for benzene catalytic oxidation on the Pt(111) surface in pressures of flowing oxygen. The intermediates with increasing temperature are  $\eta^6$ -benzene (150 K), 1,1,4-tri- $\sigma$ -2,5-cyclohexadiene (285 K), and  $\eta^5$ -cyclohexadienone (370 K).

has been calculated for benzene adsorbed on the Ag(110) surface, and this tilt has been ascribed to an inhomogeneous layer.<sup>37</sup> For a saturated coverage of benzene adsorbed on the Pd(111) surface, a tilt angle of  $30^\circ$  has been observed.<sup>43</sup> The result reported here more likely indicates that the aromatic system has rehybridized upon adsorption, which is also supported by calculations for the C–H bond angle. This bond angle is estimated by this work to be  $46^\circ \pm 5^\circ$  from the surface normal, or  $44^\circ \pm 5^\circ$  from the surface plane. Previous NEXAFS experiments and calculations have suggested that a tilt angle of up to  $40^\circ$  from the surface for the C–H bond was possible due to molecular rehybridization.<sup>44</sup> It has been proposed that the formation of metal–carbon bonds through surface interactions could perturb the NEXAFS spectra of the adsorbed benzene.<sup>45</sup> HREELS has shown that the CH-out-of-plane bending mode increases in frequency considerably, which indicates a strong interaction between the Pt(111) surface and adsorbed benzene.<sup>15</sup> Additionally, calculations using extended Hückel theory (EHT) have predicted that benzene is strongly adsorbed at both bridge and 3-fold hollow sites on the Pt(111) surface and undergoes molecular distortion.<sup>23</sup> This strong interaction between benzene and the Pt(111) surface clearly affects the molecular structure, which in turn affects the surface reactivity.

A mechanism for the catalytic oxidation of benzene on the Pt(111) surface has been developed and is presented in Figure 7. As mentioned previously, coverage estimates based on a saturated coverage of CO show that a saturated coverage of benzene consists of  $2.58 \times 10^{14}$  molecules/cm<sup>2</sup>, which agrees with previous experimental results.<sup>16–17,19,22</sup> During the initial step of the mechanism from 150 to 285 K, strongly adsorbed benzene first forms a 1,4-di- $\sigma$ -2,5-cyclohexadiene intermediate, then a 1,1,4-tri- $\sigma$ -2,5-cyclohexadiene intermediate. The formation of these intermediates is most clearly seen in Figures 4 and 5. The initial rate of carbon removal, as observed in Figure 2, is slow and primarily corresponds to desorption of benzene based on comparisons with TPRS. For the condition of excess benzene on the surface, as seen in the mass 78 spectrum in Figure 3, benzene desorption from 3-fold hollow sites is complete by 400 K. For the TP-FYNES experiments, benzene

adsorbed on 3-fold hollow sites should be completely desorbed by 370 K. (A decrease in heating rate from 5 K/s to 0.5 K/s results in a temperature decrease of 30 K, assuming first-order desorption.<sup>46</sup>) As seen in Figure 3, above 300 K benzene is oxidized to form CO<sub>2</sub> and H<sub>2</sub>O. Reaction-limited peaks for both products are observed from 300 to 500 K, which clearly indicates that oxydehydrogenation and skeletal oxidation are both occurring over this temperature range. During TP-FYNES, benzene desorption and surface reaction to form carbon dioxide and water appear to occur simultaneously from 270 K until 370 K, when the surface reaction becomes rapid. Carbon–hydrogen and carbon–carbon bond activation are clearly rate-limiting steps for carbon dioxide and water formation. Similar reactivity was observed on the Pt(111) surface under UHV conditions.<sup>30</sup>

In the initial step of the mechanism, the aromatic ring rearranges to form a 1,4-di- $\sigma$ -2,5-cyclohexadiene intermediate below 215 K, as indicated by the results presented in Figure 4. Similar species have been observed for low benzene coverages on the Pd(111) and Pt(110) surfaces using HREELS.<sup>47–48</sup> It is likely that benzene adsorbed on bridge sites rearranges to this  $\eta^2$ -diene in which two carbon atoms in para positions are bonded to the surface and the ring has buckled upward, as suggested for the Pd(111) surface.<sup>47</sup> This result would be consistent with the buckling distortion on the Pt(111) surface observed using diffuse LEED.<sup>20</sup> As shown in Figure 5, above 215 K this surface species reacts with oxygen to produce a C<sub>6</sub>H<sub>5</sub> dehydrogenated intermediate, 1,1,4-tri- $\sigma$ -2,5-cyclohexadiene, by 285 K. This dehydrogenated 1,1,4-tri- $\sigma$ -2,5-cyclohexadiene intermediate is stable until 370 K, where it then rapidly reacts with atomic oxygen on the surface. Results from FYNES shown in Figure 6 indicate that above 370 K the intermediate that undergoes rapid oxidation is  $\eta^5$ -cyclohexadienone. As reported here and elsewhere, we find no evidence for extensive decomposition of the carbon ring prior to complete oxidation.<sup>30</sup> Comparison of the spectrum in Figure 6 with those for quinoid molecules and phenoxide adsorbed on Mo(110) and Ag(110) suggests the formation of a  $\eta^5$ -cyclohexadienone intermediate.<sup>37,41–42,49</sup> This intermediate has also been proposed on the basis of HREELS of the decomposition of phenol on Pt(111).<sup>40</sup>

Previous studies using TPRS for the reaction of benzene with coadsorbed molecular oxygen showed that preadsorption of oxygen inhibits adsorption of benzene on 3-fold hollow sites.<sup>30</sup> In the experiments reported here, inhibition of oxygen adsorption by benzene is clearly seen. Oxygen has been shown to adsorb on 3-fold hollow sites on the Pt(111) surface.<sup>50–51</sup> The preadsorption of benzene inhibits the adsorption of oxygen, and as a result oxidation is inhibited. This effect has also been observed with a supported platinum catalyst.<sup>11</sup> The desorption rate for benzene does not depend on the oxygen pressure, nor does the surface reaction rate since the surface reaction above 370 K is fast. As a result, no change in the rate of surface carbon removal, or the onset temperature for rapid oxidation, is observed over the oxygen pressure range of 0.0005 to 0.01 Torr. At high oxygen concentrations no pressure dependence on the oxidation rate was observed for a platinum catalyst.<sup>12</sup> Zero-order kinetics for the oxygen concentration has also been reported for the catalytic oxidation of several alkanes on platinum foil.<sup>52</sup> Yet, a nonzero-order dependence on oxygen pressure has been observed for propylene catalytic oxidation on the Pt(111) surface over the same pressure range used in this work.<sup>31</sup> In this case, the onset temperature for rapid oxidation decreased with an increase in oxygen pressure.

Deep oxidation of benzene on the Pt(111) surface proceeds through a bimolecular surface reaction. A series of strongly

adsorbed, benzene-derived intermediates and atomic oxygen are the reacting species on the surface. Benzene strongly adsorbed on bridge sites rearranges to form a diene, which then undergoes oxydehydrogenation. Over this temperature range, the dominant surface species are both benzene and the diene intermediate. As mentioned before, preadsorption of benzene on 3-fold hollow sites completely inhibits the adsorption of oxygen, which inhibits oxidation below 370 K. Based on TP-FYNES and TPRS results reported here, inhibition will become an important factor over the 320 to 370 K temperature range depending on reaction conditions. The adsorption and dissociation of oxygen on the Pt(111) surface are not rate-limiting steps as indicated by the zero-order dependence in oxygen. The rate-limiting steps are clearly carbon–hydrogen and carbon–carbon bond activation, as reported previously for benzene oxidation under UHV conditions.<sup>30</sup> Once benzene has desorbed from 3-fold hollow sites, the oxygenated intermediate is formed and is rapidly oxidized.

## Conclusions

Benzene catalytic oxidation on the Pt(111) surface has been characterized using a combination of soft X-ray absorption spectroscopies at the C-K-edge. A mechanism has been developed using both UHV and in-situ elevated-pressure experiments. As shown by spectroscopic and temperature-programmed kinetic measurements, the reaction proceeds through four surface intermediates:  $\eta^6$ -benzene, 1,4-di- $\sigma$ -2,5-cyclohexadiene, 1,1,4-tri- $\sigma$ -2,5-cyclohexadiene, and  $\eta^5$ -cyclohexadienone. Below 150 K, benzene is adsorbed on the Pt(111) surface with the aromatic ring rehybridized and the C–H bonds at angles of  $44^\circ \pm 5^\circ$  from the surface plane. In the first step of the mechanism, from 150 to 215 K, the aromatic ring rearranges to produce a 1,4-di- $\sigma$ -2,5-cyclohexadiene surface intermediate with C<sub>6</sub>H<sub>6</sub> stoichiometry. Next, dehydrogenation over the temperature range 215 to 285 K forms a 1,1,4-tri- $\sigma$ -2,5-cyclohexadiene surface intermediate with C<sub>6</sub>H<sub>5</sub> stoichiometry.

As determined by TPRS, weakly adsorbed benzene is desorbed from 3-fold hollow sites on the surface in this same temperature range. Below 370 K benzene oxidation is inhibited by the adsorption of benzene on 3-fold hollow sites, which prevents oxygen adsorption. However, carbon dioxide and water formation is slowly occurring through a parallel deep oxidation channel over the temperature range 350 K to 370 K. In this same temperature range, a  $\eta^5$ -cyclohexadienone intermediate with C<sub>6</sub>H<sub>5</sub>O stoichiometry, which is dominant at 390 K, is produced by oxygenation. This reactive intermediate is rapidly oxidized with increasing temperature. Above 370 K, carbon dioxide and water have been identified as the gas-phase products of oxidation on Pt(111) using TPRS. This detailed mechanistic picture of benzene catalytic oxidation on the Pt(111) surface illustrates the capabilities of these coupled UHV surface science experiments and in-situ soft X-ray methods. Current efforts are underway to characterize benzene catalytic oxidation on more complex model surfaces, such as Pt thin films and nanoparticulate catalysts.

**Acknowledgment.** Financial support was provided by DOE Grant DE-FG02-91ER1490. A. L. Marsh acknowledges the National Science Foundation for support through an IGERT fellowship (Grant DGE-9972776). Part of this research was carried out at the National Synchrotron Light Source, Brookhaven National Laboratory, which is supported by the U.S. Department of Energy, Division of Materials Sciences and Division of Chemical Sciences, under Contract No. DE-AC02-98CH10886.



Certain commercial names are identified in this paper for the purpose of clarity in the presentation. Such identification does not imply endorsement by the National Institute of Standards and Technology.

## References and Notes

- (1) Thomas, J. M.; Thomas, W. J. *Principles and Practice of Heterogeneous Catalysis*; VCH Publishers: New York, 1997.
- (2) Somorjai, G. A. *Introduction to Surface Chemistry and Catalysis*; John Wiley & Sons: New York, 1994.
- (3) Goodman, D. W. *J. Phys. Chem. B* **1996**, *100*, 13090.
- (4) Somorjai, G. A.; Rupprechter, G. *J. Phys. Chem. B* **1999**, *103*, 1623.
- (5) Ertl, G. *J. Mol. Catal. A* **2002**, *182–183*, 5.
- (6) Spivey, J. J. *Ind. Eng. Chem. Res.* **1987**, *26*, 2165.
- (7) Gangwal, S. K.; Mullins, M. E.; Spivey, J. J.; Caffrey, P. R.; Tichenor, B. A. *Appl. Catal.* **1988**, *36*, 231.
- (8) Barresi, A. A.; Baldi, G. *Chem. Eng. Sci.* **1992**, *47*, 1943.
- (9) Barresi, A. A.; Mazzarino, I.; Baldi, G. *Can. J. Chem. Eng.* **1992**, *70*, 286.
- (10) Ordóñez, S.; Bello, L.; Sastre, H.; Rosal, R.; Díez, F. V. *Appl. Catal. B* **2002**, *38*, 139.
- (11) Garetto, T. F.; Apesteguía, C. R. *Appl. Catal. B* **2001**, *32*, 83.
- (12) de Jong, V.; Cieplik, M. K.; Reints, W. A.; Fernandez-Reino, F.; Louw, R. *J. Catal.* **2002**, *211*, 355.
- (13) Grin, S. A.; Sergeeva, T. U.; Tenyanko, N. V.; Gaidai, N. A.; Gudkov, B. S.; Dryakhlov, A. S.; Kiperman, S. L. In *Heterogeneous Catalysis: Proceedings of the Sixth International Symposium, Part 1*; Shopov, D., Andreev, A., Palazov, A., Petrov, L., Eds.; Publishing House of the Bulgarian Academy of Sciences: Sofia, 1987.
- (14) Tenyanko, N. V.; Sergeeva, T. Y.; Gaidai, N. A.; Gudkov, B. S.; Dryakhlov, A. S.; Kiperman, S. L. *Kinet. Catal.* **1990**, *31*, 340.
- (15) Lehwald, S.; Ibach, H.; Demuth, J. E. *Surf. Sci.* **1978**, *78*, 577.
- (16) Tsai, M.-C.; Muetterties, E. L. *J. Am. Chem. Soc.* **1982**, *104*, 2534.
- (17) Abon, M.; Bertolini, J. C.; Billy, J.; Massardier, J.; Tardy, B. *Surf. Sci.* **1985**, *162*, 395.
- (18) Horsley, J. A.; Stöhr, J.; Hitchcock, A. P.; Newbury, D. C.; Johnson, A. L.; Sette, F. *J. Chem. Phys.* **1985**, *83*, 6099.
- (19) Campbell, J. M.; Seimanides, S.; Campbell, C. T. *J. Phys. Chem.* **1989**, *93*, 815.
- (20) Wander, A.; Held, G.; Hwang, R. Q.; Blackman, G. S.; Xu, M. L.; de Andres, P.; Van Hove, M. A.; Somorjai, G. A. *Surf. Sci.* **1991**, *249*, 21.
- (21) Weiss, P. S.; Eigler, D. M. *Phys. Rev. Lett.* **1993**, *71*, 3139.
- (22) Xu, C.; Tsai, Y.-L.; Koel, B. E. *J. Phys. Chem.* **1994**, *98*, 585.
- (23) Minot, C.; Van Hove, M. A.; Somorjai, G. A. *Surf. Rev. Lett.* **1995**, *2*, 285.
- (24) Haq, S.; King, D. A. *J. Phys. Chem.* **1996**, *100*, 16957.
- (25) Saeys, M.; Reyniers, M.-F.; Marin, G. B.; Neurock, M. *J. Phys. Chem. B* **2002**, *106*, 7489.
- (26) Guo, X.-C.; Madix, R. J. *Catal. Lett.* **1996**, *39*, 1.
- (27) Walton, R. M. *Mechanistic Studies of Platinum-Titania and Platinum-Alumina Thin Films for Microchemical Gas Sensors*. Ph.D. Dissertation, University of Michigan, Ann Arbor, MI, 1997.
- (28) Harris, T. D.; Madix, R. J. *J. Catal.* **1998**, *178*, 520.
- (29) Viste, M. E.; Gibson, K. D.; Sibener, S. J. *J. Catal.* **2000**, *191*, 237.
- (30) Marsh, A. L.; Gland, J. L. *Surf. Sci.* **2003**, *536*, 145.
- (31) Gabelnick, A. M.; Capitano, A. T.; Kane, S. M.; Gland, J. L.; Fischer, D. A. *J. Am. Chem. Soc.* **2000**, *122*, 143.
- (32) Gabelnick, A. M.; Burnett, D. J.; Gland, J. L.; Fischer, D. A. *J. Phys. Chem. B* **2001**, *105*, 7748.
- (33) Burnett, D. J. In *Situ Mechanistic Studies of the Oxidation of Carbon Monoxide, Ethylene, and Acetylene over Platinum Surfaces*. Ph.D. Dissertation, University of Michigan, Ann Arbor, MI, 2001.
- (34) Fischer, D. A.; Colbert, J.; Gland, J. L. *Rev. Sci. Instrum.* **1989**, *60*, 1596.
- (35) Norton, P. R.; Davies, J. A.; Jackman, T. E. *Surf. Sci.* **1982**, *122*, L593.
- (36) Outka, D. A.; Stöhr, J. *J. Chem. Phys.* **1988**, *88*, 3539.
- (37) Solomon, J. L.; Madix, R. J.; Stöhr, J. *Surf. Sci.* **1991**, *255*, 12.
- (38) Stöhr, J.; Outka, D. *Phys. Rev. B* **1987**, *36*, 7891.
- (39) Stöhr, J. *NEXAFS Spectroscopy*; Gomer, R., Ed.; Springer Series in Surface Science 25; Springer: New York, 1992.
- (40) Ihm, H.; White, J. M. *J. Phys. Chem. B* **2000**, *104*, 6202.
- (41) Francis, J. T.; Hitchcock, A. P. *J. Phys. Chem.* **1992**, *96*, 6598.
- (42) Bäessler, M.; Fink, R.; Buchberger, C.; Väterlein, P.; Jung, M.; Umbach, E. *Langmuir* **2000**, *16*, 6674.
- (43) Hoffmann, H.; Zaera, F.; Ormerod, R. M.; Lambert, R. M.; Wang, L. P.; Tysse, W. T. *Surf. Sci.* **1990**, *232*, 259.
- (44) Mainka, C.; Bagus, P. S.; Schertel, A.; Strunskus, T.; Grunze, M.; Wöll, Ch. *Surf. Sci.* **1995**, *341*, L1055.
- (45) Liu, A. C.; Stöhr, J.; Friend, C. M.; Madix, R. J. *Surf. Sci.* **1990**, *235*, 107.
- (46) Redhead, P. A. *Vacuum* **1962**, *12*, 203.
- (47) Grassian, V. H.; Muetterties, E. L. *J. Phys. Chem.* **1987**, *91*, 389.
- (48) Chen, N. S.; Ford, L. P.; Masel, R. I. *Catal. Lett.* **1998**, *56*, 105.
- (49) Liu, A. C.; Friend, C. M.; Stöhr, J. *Surf. Sci.* **1990**, *236*, L349.
- (50) Steininger, H.; Lehwald, S.; Ibach, H. *Surf. Sci.* **1982**, *123*, 1.
- (51) Starke, U.; Materer, N.; Barbieri, A.; Döll, R.; Heinz, K.; Van Hove, M. A.; Somorjai, G. A. *Surf. Sci.* **1993**, *287–288*, 432.
- (52) Aryafar, M.; Zaera, F. *Catal. Lett.* **1997**, *48*, 173.